Clinical usefulness of right ventricular 3D area strain in the assessment of treatment effects of balloon pulmonary angioplasty in chronic thromboembolic pulmonary hypertension: Comparison with 2D feature-tracking MRI

Kawakubo, Masateru
Department of Health Sciences, Faculty of Medical Sciences, Kyushu University: Assistant Professor

Yamasaki, Yuzo
Department of Clinical Radiology, Graduate School of Medical Sciences, Kyushu University

Kamitani, Takeshi
Department of Clinical Radiology, Graduate School of Medical Sciences, Kyushu University

Sagiyama, Koji
Department of Clinical Radiology, Graduate School of Medical Sciences, Kyushu University

他

出版情報：European radiology. 29 (9), pp.4583-4592, 2019-09-01. European Society of Radiology
バージョン：
権利関係：

Clinical usefulness of right ventricular 3D area strain in the assessment of treatment effects of balloon pulmonary angioplasty in chronic thromboembolic pulmonary hypertension: Comparison with 2D feature-tracking MRI

Masateru Kawakubo, PhD

k-mstr@hs.med.kyushu-u.ac.jp

Department of Health Sciences, Faculty of Medical Sciences, Kyushu University

3-1-1 Maidashi, Higashi-ku Fukuoka-shi, Fukuoka, Japan

Yuzo Yamasaki, MD

yyama@radiol.med.kyushu-u.ac.jp

Department of Clinical Radiology, Graduate School of Medical Sciences, Kyushu University

3-1-1 Maidashi, Higashi-ku Fukuoka-shi, Fukuoka, Japan

Takeshi Kamitani, MD

kamitani@radiol.med.kyushu-u.ac.jp

Department of Clinical Radiology, Graduate School of Medical Sciences, Kyushu University

3-1-1 Maidashi, Higashi-ku Fukuoka-shi, Fukuoka, Japan

Koji Sagiyama, MD

sagiyama@radiol.med.kyushu-u.ac.jp

Department of Clinical Radiology, Graduate School of Medical Sciences, Kyushu University

3-1-1 Maidashi, Higashi-ku Fukuoka-shi, Fukuoka, Japan

Yuko Matsuura, MD

urarisu@yahoo.co.jp

Department of Clinical Radiology, Graduate School of Medical Sciences, Kyushu University

3-1-1 Maidashi, Higashi-ku Fukuoka-shi, Fukuoka, Japan

Takuya Hino, MD

Takuya.9.26.8@gmail.com

Department of Clinical Radiology, Graduate School of Medical Sciences, Kyushu University

3-1-1 Maidashi, Higashi-ku Fukuoka-shi, Fukuoka, Japan

Kohtaro Abe, MD

koabe@cardiol.med.kyushu-u.ac.jp

Department of Cardiovascular Medicine, Graduate School of Medical Sciences, Kyushu University

3-1-1 Maidashi, Higashi-ku Fukuoka-shi, Fukuoka, Japan

Kazuya Hosokawa, MD

ncvchoso@cardiol.med.kyushu-u.ac.jp

Department of Cardiovascular Medicine, Graduate School of Medical Sciences, Kyushu University

3-1-1 Maidashi, Higashi-ku Fukuoka-shi, Fukuoka, Japan

Hidetake Yabuuchi, MD

h-yabu@hs.med.kyushu-u.ac.jp

Department of Health Sciences, Faculty of Medical Sciences, Kyushu University

3-1-1 Maidashi, Higashi-ku Fukuoka-shi, Fukuoka, Japan

Hiroshi Honda, MD

honda@radiol.med.kyushu-u.ac.jp

Department of Clinical Radiology, Graduate School of Medical Sciences, Kyushu University

3-1-1 Maidashi, Higashi-ku Fukuoka-shi, Fukuoka, Japan

Author for correspondence:

Masateru Kawakubo, PhD

Department of Health Sciences, Faculty of Medical Sciences, Kyushu University

3-1-1 Maidashi Higashi-ku Fukuoka 812-8582, Japan

Tel: +81-92-642-6728

Fax: +81-92-642-6728

E-mail: k-mstr@hs.med.kyushu-u.ac.jp

Clinical usefulness of right ventricular 3D area strain in the assessment of treatment effects of balloon pulmonary angioplasty in chronic thromboembolic pulmonary hypertension: Comparison with 2D feature-tracking MRI

Abstract (230 / 250 words)

Objectives

To evaluate the usefulness of right ventricular (RV) area strain analysis via cardiac MRI (CMRI) as a tool for assessing the treatment effects of balloon pulmonary angioplasty (BPA) in inoperable chronic thromboembolic pulmonary hypertension (CTEPH), RV area strain was compared to two-dimensional (2D) strain with feature-tracking MRI (FTMRI) before and after BPA.

Methods

We retrospectively analyzed 21 CTEPH patients who underwent BPA. End-systolic global area strain (GAS), longitudinal strain (LS), circumferential strain (CS), and radial strain (RS) were measured before and after BPA. Changes in GAS and RV ejection fraction (RVEF) values after BPA were defined as

ΔGAS and ΔRVEF. Receiver operating characteristic (ROC) analyses were performed to determine the optimal cutoff of the strain at after BPA for detection of improved patients with decreased mean pulmonary artery pressure (mPAP) less than 30 mmHg and increased RVEF more than 50 %.

Results

ROC analysis revealed the optimal cutoffs of strains (GAS, LS, CS, and RS) for identifying improved patients with mPAP<30 mmHg (cutoff (%) = -41.2, -13.8, -16.7, and 14.4: area under the curve, 0.75, 0.56, 0.65, and 0.75) and patients with RVEF>50 % (cutoff (%) = -37.2, -29.5, -2.9, and 14.4: area under the curve, 0.81, 0.60, 0.56, and 0.56).

Conclusions

Area strain analysis via CMRI may be a more useful tool for assessing the treatment effects of BPA in patients with CTEPH than 2D strains with FTMRI.

Keywords (3 to 5)

Myocardial Contraction, Balloon Angioplasty, Cine Magnetic Resonance Imaging, Pulmonary Heart Disease, Right Ventricle

Key points (1 to 3)

- Area strain values can detect improvement of right ventricular (RV) pressure and function after balloon pulmonary angioplasty (BPA) equally or more accurately than two-dimensional strains.
- Area strain analysis is a useful analytical method that reflects improvements in complex RV myocardial deformation by BPA.
- Area strain analysis is a robust method with reproducibility equivalent to that of 2D strain analysis.

Abbreviations

CTEPH: chronic thromboembolic pulmonary hypertension

BPA: balloon pulmonary angioplasty

RV: right ventricular

CMRI: cardiac magnetic resonance imaging

FTMRI: feature-tracking magnetic resonance imaging

2D: two-dimensional

3D: three-dimensional

RHC: right heart catheterization

mPAP: mean pulmonary artery pressure

SSFP: steady-state free precession

TR: repetition time

TE: echo time

LV: left ventricular

EDV: end-diastolic volume

ESV: end-systolic volume

EF: ejection fraction

SVi: stroke volume index

CI: cardiac index

LS: longitudinal strain

CS: circumferential strain

RS: radial strain

GAS: global area strain

AS_{base}: basal area strain

AS_{mid}: middle area strain

AS_{apex}: apical area strain

IQR: inter quartile range

PVR: pulmonary vascular resistance

6MWD: 6-minute walking distance

BNP: brain natriuretic peptide

ROC: receiver operating characteristic

ICC: intraclass correlation coefficient

TAPSE: tricuspid annular plane systolic excursion

IVS: interventricular septum

Introduction

Chronic thromboembolic pulmonary hypertension (CTEPH) is a fatal disease characterized by thrombotic occlusion or narrowing of the pulmonary arteries resulting in pulmonary hypertension, right-side heart failure, and death [1,2]. Balloon pulmonary angioplasty (BPA) is a promising option for inoperable patients with CTEPH [3]. Considering that clinical parameters of right ventricular (RV) function are associated with prognosis, RV reverse remodeling, pulmonary pressure overload, and interventricular dyssynchrony in patients with CTEPH [4–8], noninvasive evaluation of RV function is paramount to accurately assess the effects of treatment during repeated BPA sessions. Echocardiographic strain imaging, such as tissue Doppler imaging and speckle tracking, is widely used in clinical examination for the assessment of myocardial function [9]. However, the echocardiographic strain imaging of the right ventricle has historically been challenging due to its complex morphology, thin wall with coarse trabeculations, and anterior position within the chest.

Recent developments in cardiac MRI (CMRI) have enabled image-based assessment of RV

function, and CMRI is currently considered the reference standard [10]. Feature-tracking MRI (FTMRI) enables tracking of tissue voxel motion using only standard two-dimensional (2D) cine MRI and the evaluation of wall mechanics and strains without the need for acquisition of additional sequences [11–14]. However, a fixed 2D slice plane lacks visual information pertaining to original myocardial features that is yielded by frame-by-frame tracking analysis [15]. Therefore, three-dimensional (3D) image-based analysis has a theoretical advantage compared to 2D analysis. Global and regional area strain determined via echocardiography, which quantifies 3D changes in the endocardial surface area, have been reported as sensitive predictors of myocardial damage [16,17]. To the best of our knowledge, there is no report describing the analysis of RV area strain via CMRI for assessing the treatment effects of BPA in patients with CTEPH. In the present study, we measured changes in 3D area strain and 2D strain before and after BPA to investigate the extent to which area strain analysis may constitute a useful tool for assessing the treatment effects of BPA, when compared to 2D strains assessed by FTMRI. We also inspected correlations between the changes of strains and physiological indices and RV function.

Materials and methods

Study population

This retrospective observational study was approved by our institutional review board, and written informed consent was obtained from each patient. Twenty-one patients with CTEPH were enrolled in the study, and datasets derived between May 2012 and December 2017 were analyzed. Inclusion criteria were being older than 20 years and in a clinically stable state. Diagnosis of CTEPH and eligibility for BPA were determined according to previously reported procedures and criteria [18,19]. To exclude left-side heart disease and pulmonary disease, all patients received echocardiography and high resolution computed tomography. All BPAs were performed in the peripheral pulmonary arteries and multiple pulmonary arterial lesions were dilated in the same BPA session. All patients underwent the first right heart catheterization (RHC) within 1 month before the first BPA session. Post-operative hemodynamic measurements were assessed 1 and 6 months after the last BPA session. CMRIs were performed within 1

month before the first BPA session and within 1 month after the last BPA session, when the mean pulmonary artery pressure (mPAP) had decreased less than 30mmHg.

Cine MR imaging

CMRI was performed using a 3.0-T clinical scanner (Achieva 3.0 T Quasar Dual; Philips Healthcare), equipped with dual-source parallel radiofrequency transmission and a cardiac phased array 32-channel receiver coil. Cine steady-state free precession (SSFP) images were obtained using a multi-breath holding (approximately 10–20 s) SSFP sequence, with retrospective electrocardiogram gating in the 4-chamber view and in contiguous short-axis views covering the whole left ventricle and right ventricle with approximately 10 images and with 20 phases per cardiac cycle. The cine imaging parameters were repetition time (TR) 2.8 ms, echo time (TE) 1.4 ms, SENSE factor 2.0, flip angle 45°, slice thickness 8 mm, slice gap 0 mm, field of view 380 × 380 mm2, acquisition matrix 176 × 193, and reconstruction matrix 352 × 352. RV volume analysis was performed semi-automatically with subsequent manual correction using a workstation (IntelliSpace Portal, Philips Healthcare). RV volumes were measured on

the basis of axial images as previous report [20]. Left ventricular (LV) volumes were measured on the basis of short-axis images. End-diastolic volume (EDV) and end-systolic volume (ESV) were indexed to the body surface area, and these values were designated EDVi and ESVi. The ejection fraction (EF) was calculated via EDV and ESV. Stroke volume index (SVi) was calculated as the difference between EDVi and ESVi. Cardiac index (CI) was the product of SVi and heart rate.

Strain analysis using 2D cine MRI

Myocardial strain was analyzed semi-automatically with subsequent manual correction using an in-house original off-line feature-tracking tool that has been validated in a previous clinical study [21]. This algorithm was designed using MATLAB R2017b version 9.3 (The Mathworks Inc., Massachusetts). First, endocardial borders, including the ventricular septum, were manually defined as some arbitrary points at the end of diastole. The endocardium points were then tracked for a cardiac cycle with a local template-matching technique based on normalized correlation coefficient values. Lastly, the strain values for a cardiac cycle were automatically calculated from the coordinates of each point. End-systolic

longitudinal strain (LS), circumferential strain (CS), and radial strain (RS) were defined as the peak value of each strain. CS and RS analyses were performed based on short-axis cine imaging in the middle of the right ventricle, and LS analysis was performed via four-chamber cine imaging.

Area strain analysis with 2D cine MRI

Area strain analyses were conducted using MATLAB-based manual segmentation of the RV surface. On the short-axis cine image, the endocardial surface of the right ventricle, including ventricular septum, was manually delineated as lines for a cardiac cycle (Fig. 1A). The delineated lines were plotted on 3D coordinates (Fig. 1B). Endocardial area of the whole RV was calculated from these lines by spline interpolation for each time phase (Fig. 1C). The endocardial area was then segmented into basal, middle, and apical regions by dividing the ventricle cavity in three equal longitudinal length segments (Fig. 1D). These segmentations were performed for each time phase during one cardiac cycle. During RV contraction, the endocardial surface area decreases in size because of longitudinal and circumferential shortening and radial myocardial thickening [17]. Area strain reflects this change in the endocardial

surface area (Area(t)), and provides a quantitative metric representing the percentage change in area from its original dimensions (Area(D)), calculated as per below:

$$Area\ strain(\%) = \frac{Area(t) - Area(D)}{Area(D)} \times 100$$

The end-systolic global area strain (GAS) and basal, middle, and apical area strain (AS_{base}, AS_{mid}, and AS_{apex}) were the minimum peak area of each area strain (Fig. 1E).

Statistically analysis

The Shapiro-Wilk test was employed to assess normality of data distribution. Due to non-normal data distribution, descriptive statistics are provided as median and the corresponding inter quartile ranges (IQR). The area strain values GAS, AS_{base}, AS_{mid}, and AS_{apex} and the LS, CS, and RS values before and after BPA were compared using the Wilcoxon signed-rank test. Changes in strain values (GAS, AS_{base}, AS_{mid}, and AS_{apex}, as well as LS, CS, and RS), mPAP, pulmonary vascular resistance (PVR), 6-minute walking distance (6MWD), brain natriuretic peptide (BNP), RVEDVi, RVESVi, and RVEF before and after BPA were defined as ΔGAS, ΔAS_{base}, ΔAS_{mid}, ΔAS_{apex}, ΔLS, ΔCS, ΔRS, ΔmPAP, ΔPVR, Δ6MWD,

ΔBNP, ΔRVEDVi, ΔRVESVi, and ΔRVEF. Receiver operating characteristic (ROC) analyses were performed to determine the optimal cutoff of the strain for detection of improved patients after BPA, defined as: mPAP<30 mmHg [22], BNP<18.4 pg/mL [23], and RVEF>50 % [24]. The differences of ROCs of AS_{base}, AS_{mid}, and AS_{apex} were tested against each other by DeLong's test. Correlations between changes in strain values (ΔGAS, ΔAS_{base}, ΔAS_{mid}, ΔAS_{apex}, ΔLS, ΔCS, and ΔRS) and changes in clinical indices (ΔmPAP, ΔPVR, Δ6MWD, and ΔBNP) after BPA were calculated using Spearman's rank correlation coefficient (ρ). Similarly, ρ values were calculated between changes in strain values and changes in RV volumetric parameters (ΔRVEDVi, ΔRVESVi, and ΔRVEF). Correlations between strains (GAS, AS_{base}, AS_{mid}, and AS_{apex}, as well as LS, CS, and RS) and RVEF were calculated before and after BPA. All statistical analyses were conducted using the SAS software for Windows (version 13, SAS Inc.). Statistical significance was set at $p < 0.05$.

Intra- and inter-observer reproducibility

All 2D and 3D strain measurements were tested for intra-observer reproducibility by having one

observer performing all GAS analyses on 10 randomly selected patients, 5 in the before BPA group and 5 in the after BPA group, then blindly repeating the analyses on a separate occasion. Inter-observer reproducibility was evaluated by a second observer blinded to the clinical and experimental data, performing GAS measurements on the same 10 patients. Intra- and inter-observer reproducibility of the measurements of GAS, AS_{base}, AS_{mid}, AS_{apex}, CS, LS, and RS were evaluated using Bland-Altman analyses and intraclass correlation coefficient (ICC) with one-way random single measures or two-way random single measures (ICC(1, 1) or ICC(2,1)). ICCs were defined as excellent (ICC $\geq$ 0.75), good (ICC = 0.60 - 0.74), moderate (ICC = 0.40 - 0.59) and poor (ICC $\leq$ 0.39).

Results

Baseline clinical characteristics and BPA procedure are shown in Table 1. BPA procedures were successfully performed in all patients. Hemodynamic and laboratory data and CMRI characteristics of the study population are shown in Table 2. The clinical indices of mPAP, PVR, 6MWD, and BNP were

significantly improved after BPA. The RV functions RVEDVi, RVESVi, and RVEF as measured via CMRI were also significantly improved after BPA. The LV function was preserved and stable before and after BPA. Table 3 shows the 2D strains and area strains before and after BPA. GAS, AS_{base}, AS_{apex}, LS, and RS were significantly improved after BPA.

ROC analysis was used to describe the optimal cutoffs of 3D strains (GAS, AS_{base}, AS_{mid}, and AS_{apex}) and 2D strains (LS, CS, and RS) in order to identify improved patients with mPAP <30 mmHg, BNP <18.4 pg/mL, and RVEF >50% (shown in Table 4).~~ROC analysis described the optimal cutoffs of 3D strains (GAS, AS_{base}, AS_{mid}, and AS_{apex}) for identifying improved patients with mPAP<30 mmHg (cutoff (%) = -41.2, -46.3, -45.3, and -51.8: area under the curve, 0.75, 0.84, 0.74, and 0.45; sensitivity, 0.20, 0.20, 0.20, and 0.00; specificity, 1.00 for all) (Fig. 2A), and described those of 2D strains (LS, CS, and RS) in Figure 2B (cutoff (%) = -13.8, -16.7, and 14.4: area under the curve, 0.56, 0.65, and 0.75; sensitivity, 0.00, 0.20, and 0.00; specificity, 1.00 for all). Similarly, the identifying abilities of 3D strains for patients with BNP<18.4 pg/mL were cutoff (%) = -37.5, -31.8, -33.2, and -42.1: area under the~~

~~curve, 0.53, 0.75, 0.65, and 0.63; sensitivity, 1.00, 0.78, 0.67, and 0.67; specificity, 0.33, 0.67, 0.67, and 0.75 (Fig. 2C), and those of 2D strains were cutoff (%) = -21.7, -14.4, and 12.7: area under the curve, 0.55, 0.53, and 0.51; sensitivity, 0.56, 0.33, and 1.00; specificity, 0.67, 0.83, and 0.33 (Fig. 2D). The identifying abilities of 3D strains for patients with RVEF>50 % were cutoff (%) = -37.2, -42.8, -45.3, and -51.8: area under the curve, 0.81, 0.81, 0.66, and 0.65; sensitivity, 0.88, 1.00, 1.00, and 1.00; specificity, 0.75, 0.25, 0.00, and 0.00 (Fig. 2E), and those of 2D strains were cutoff (%) = -29.5, -2.9, and 14.4: area under the curve, 0.60, 0.56, and 0.56; sensitivity, 1.00 for all; specificity, 0.00 for all (Fig. 2F).~~ There were significant differences only between the ROC curves of AS_{base} and AS_{apex} in all comparisons ($p = 0.02$). Spearman's rank correlations between changes in strain values and changes in clinical indices and between changes in strain values and changes in RV volumetric parameters after BPA are shown in Table 5. The ΔGAS was significantly correlated with ΔBNP, ΔRVESVi, and ΔRVEF ($\rho = 0.57$, 0.61, and -0.68; $p < 0.01$ for all tested correlations). The ΔAS_{mid} was significantly correlated with ΔRVEF ($\rho = -0.52$, $p < 0.05$). The ΔAS_{apex} was significantly correlated with ΔPVR, ΔBNP,

ΔRVEDVi, and ΔRVESVi (ρ = 0.65, 0.44, 0.46, and 0.56; $p < 0.01$, $p < 0.05$, $p < 0.05$, and $p < 0.01$). The ΔLS was significantly correlated with ΔRVESVi and ΔRVEF (ρ = 0.47 and -0.44; $p < 0.05$ for all tested correlations). The ΔRS was significantly correlated with ΔRVEDVi, ΔRVESVi, and ΔRVEF (ρ = -0.51, -0.55, and -0.54; $p < 0.05$ for all tested correlations). GAS, LS, and RS were significantly correlated with RVEF (ρ = -0.66, -0.44, and 0.58; $p < 0.01$ for all tested correlations). No significant correlation between CS and RVEF could be identified (ρ = -0.20, p = 0.19) (Fig. 2). AS_{base}, AS_{mid}, and AS_{apex} were significantly correlated with RVEF (ρ = -0.54, -0.33, and 0.58; $p < 0.01$, $p < 0.05$, and $p < 0.01$).

The intra- and inter-observer reproducibility for strain analyses are shown in Table 6. Excellent intra- and inter-observer reproducibility could be observed. Bland-Altman analysis indicated small bias and standard deviation of the difference and a narrow limit of agreement. All ICCs were indicative of excellent reproducibility (ICC>0.75, $p < 0.01$).

Discussion

The current study yielded three major findings. Firstly, area strain values can detect improvement of the RV pressure (mPAP) and function (RVEF) after BPA equally or more accurately than 2D strains, possibly constituting an improved tool for assessing treatment effects of BPA. Secondly, area strain analysis is a useful analytical method that reflects improvements in complex RV myocardial deformation by BPA. Lastly, area strain analysis is a robust method with reproducibility equivalent to that of 2D strain analysis.

In the present study, area strain and 2D strain were analyzed in patients with CTEPH before and after BPA, as clinical indicators of the treatment effects of BPA. Physiological examination parameters (mPAP, PVR, 6MWD, and BNP) and RV function determined via CMRI were significantly improved after BPA. Reflecting the decrease in HR and RV volumes, there were no significant differences in SVi or CI after BPA. In the patients of present study, the period of CMRI between before and after BPA was not uniformed. Because BPA does not immediately improve hemodynamics, and it takes several weeks

to observe major effects [25]. Also the improved hemodynamics were maintained even 1year after BPA [26]. One of the main goals of this study was to investigate the clinical usefulness of area strain analysis for assessing the treatment effects of BPA, given CMRI confirmation of patients who clearly improved after treatment. Nevertheless, further studies should also investigate how useful GAS can be as a quantitative tool assessing the treatment effects of BPA during repeated sessions. Our ROC analyses support good diagnostic performance of the GAS and 2D strains measured after BPA for detecting changes to normal in the case of the mPAP (<30mmHg), the BNP (<18.4pg/mL) and the RVEF (>50%). In the analyses of mPAP and RVEF, area strain values could detect their improvement after BPA equally or more accurately than 2D strains. However, low diagnostic performance was observed in all strains for the BNP analysis – indeed, only the ΔGAS was significantly correlated the ΔBNP. Altogether, these data suggest area strain analysis may constitute an useful tool for assessing treatment effects of BPA. In the comparison of the ROC curves of 3D regional area strains (AS_{base}, AS_{mid}, and AS_{apex}), AS_{base} detected only normal change in mPAP, but the detectability in other comparisons was equivalent. In contrast,

ΔAS_{apex} was significantly correlated with ΔPVR, ΔBNP, ΔRVEDVi, and ΔRVESVi. Based on these results, we concluded that AS_{apex} is a more useful marker to assess the treatment effects of BPA.

GAS was significantly improved after BPA and correlated significantly with RVEF. It has been previously reported that LS is a sensitive marker for the evaluation of RV function [27,28]. In the present study, LS also significantly improved after BPA and correlated significantly with RVEF. There was no significant difference in the CS before and after BPA. However, sight should not be lost that previous studies have reported that the right ventricle, having a two-layer muscular fiber, deforms largely on the long axis [29] and that RV myocardium not only contracts but twists [30]. Both of these are motions towards the center of the heart, which is the middle of the ventricle. Thus, in the RV that moves largely in the long axis direction, the motion to the ventricular middle is less than to the ventricle base and apex. Considering that the CS was measured at the middle ventricular level, the motion peculiarities may underlie this result. However, we acknowledge that further investigation is needed to support or reject this hypothesis. Furthermore, an advantage of area strain with regard to RVEF is the

quantification of regional myocardial deformation. In patients with CTEPH, AS_{base} and AS_{apex} significantly improve after BPA, but AS_{mid} does not. These results are consistent with those presented by López-Candales et al.'s [31], where the authors reported on the progressive reduction in the basal and apical RV strain during chronic pulmonary hypertension. In addition to the CS, also the results of AS_{mid} may be due to the basic characteristics of the RV motion mechanism. Area strain analysis may, thus, be a useful analytical method reflecting improvements in complex RV myocardial deformation after BPA.

Importantly, we found both 3D and 2D strain analyses to exhibit excellent reproducibility in our intra- and inter-observer analysis. The reproducibility of 2D strain, as assessed via FTMRI, had been previously validated[32,33]. Therefore, we consider that area strain analysis is a robust method with equivalent reproducibility to 2D strain analysis via FTMRI. We also know that the tricuspid annular plane systolic excursion (TAPSE), evaluated through echocardiography, is a common and easy tool to assess RV function. However, the superiority of RV longitudinal strain over TAPSE had been previously reported [27,34]. These were analyses of strains of RV free walls only. In our study we aimed to move a

step forward by including strains of the interventricular septum (IVS) in all analyses. Nevertheless, one should note that the inclusion of IVS into RV mechanical analysis is a subject of intense debate. It is not clear whether free-wall and septum or only free-wall measures may be more useful as a marker of RV contractility [10,35]. It is a possible scenario that the difference between these two measurements is mostly technical. On the other hands, pulmonary hypertension is associated with a RV contraction delay. Loss of a coordinated ventricular contraction results in impaired RV systolic function. The prolonged RV contraction during early LV diastole causes the already relaxing interventricular septum to bulge into the LV. This negatively influences early LV filling, and eventually contributes to reduction of stroke volume [7]. Therefore, it seems likely that IVS may play an important role in assessment of RV function at least during pulmonary hypertension. We also note that with our method, myocardial area strain can be derived from routine MRI without additional image acquisition. This feature, along with its excellent reproducibility, strongly supports the feasibility and cost-effectiveness of our approach to be used in the clinical routine.

Limitations

Some limitations should be acknowledged. Area strain was not compared with other 3D strain parameters. The reason for this was that 3D strain analysis of RV has not been sufficiently established, and 2D evaluation is still mainstream. Although only the global 2D strains could be evaluated due to the specifications of our in-house software, area strain was compared with RV volumetric functions and strain, as determined via CMRI. Further studies should compare regional area and regional 2D strains in order to provide a more detailed picture. Another major limitation of this research is our small sample size (n = 21) and the absence of a control group. In addition to low sensitivity and specificity, there was a lack of significant differences in comparisons of AUC in ROC analyses. We suspect that these results caused the small number of patients and influenced the patient background in this study. Patients after BPA were enrolled at the endpoint of treatment (mPAP <30 mmHg). The large difference between patients with and without improved strains is a bias in the ROC analysis. We believe our approach, although promising, cannot be moved forward before evidence from further analyses with large cohorts

and inclusion of controls might be gathered.

Conclusions

Area strain analysis may be a robust and useful tool for assessing the treatment effects of BPA. Once further confirmatory evidence might be gathered, this approach is likely to constitute an improved and cost-effective tool potentially useful for the clinical examination of patients with CTEPH.

Acknowledgements

This work was supported by JSPS KAKENHI Grant Number JP16K19860 and by Kyushu University Research Activity Support Program Foreign language Proofreading Expenses Support.

References

1. Pepke-Zaba J, Delcroix M, Lang I, et al (2011) Chronic thromboembolic pulmonary hypertension (CTEPH): Results from an international prospective registry. Circulation. DOI:10.1161/CIRCULATIONAHA.110.015008

2. Moneta GL(2006) Incidence of Chronic Thromboembolic Pulmonary Hypertension After Pulmonary Embolism. Yearb Vasc Surg. DOI:10.1016/S0749-4041(08)70317-8

3. Feinstein JA, Goldhaber SZ, Lock JE, Ferndandes SM, Landzberg MJ (2001) Balloon Pulmonary Angioplasty for Treatment of Chronic Thromboembolic Pulmonary Hypertension. Circulation. DOI:10.1161/01.CIR.103.1.10

4. Fukui S, Ogo T, Morita Y, et al (2014) Right ventricular reverse remodelling after balloon pulmonary angioplasty. Eur Respir J. DOI:10.1183/09031936.00012914

5. Kamimura Y, Okumura N, Adachi S, et al (2018) Usefulness of scoring right ventricular function for assessment of prognostic factors in patients with chronic thromboembolic pulmonary

hypertension. Heart Vessels. DOI:10.1007/s00380-018-1168-7

6. Rolf A, Rixe J, Kim WK, et al (2014) Right ventricular adaptation to pulmonary pressure load in patients with chronic thromboembolic pulmonary hypertension before and after successful pulmonary endarterectomy--a cardiovascular magnetic resonance study. J Cardiovasc Magn Reson. DOI:10.1186/s12968-014-0096-7

7. Yamasaki Y, Nagao M, Abe K, et al (2017) Balloon pulmonary angioplasty improves interventricular dyssynchrony in patients with inoperable chronic thromboembolic pulmonary hypertension: a cardiac MR imaging study. Int J Cardiovasc Imaging. DOI:10.1007/s10554-016-0985-y

8. Surie S, Reesink HJ, Marcus JT, et al (2013) Bosentan treatment is associated with improvement of right ventricular function and remodeling in chronic thromboembolic pulmonary hypertension. Clin Cardiol. DOI:10.1002/clc.22197

9. Gorcsan J, Tanaka H. Echocardiographic assessment of myocardial strain (2011) J Am Coll

Cardiol. DOI:10.1016/j.jacc.2011.06.038

10. Prati G, Vitrella G, Allocca G, et al (2015) Right Ventricular Strain and Dyssynchrony Assessment in Arrhythmogenic Right Ventricular Cardiomyopathy: Cardiac Magnetic Resonance Feature-Tracking Study. Circ Cardiovasc Imaging. DOI:10.1161/CIRCIMAGING.115.003647

11. Pedrizzetti G, Claus P, Kilner PJ, Nagel E (2016) Principles of cardiovascular magnetic resonance feature tracking and echocardiographic speckle tracking for informed clinical use. J Cardiovasc Magn Reson. DOI:10.1186/s12968-016-0269-7

12. Nagao M, Yamasaki Y (2018) Cardiac Strain Analysis Using Cine Magnetic Resonance Imaging and Computed Tomography. Cardiovasc Imaging Asia. DOI:10.22468/cvia.2018.00052

13. Schuster A, Hor KN, Kowallick JT, Beerbaum P, Kutty S (2016) Cardiovascular Magnetic Resonance Myocardial Feature Tracking: Concepts and Clinical Applications. Circ Cardiovasc Imaging. DOI:10.1161/CIRCIMAGING.115.004077

14. Hor KN, Baumann R, Pedrizzetti G, et al (2011) Magnetic Resonance Derived Myocardial Strain

Assessment Using Feature Tracking. J Vis Exp. DOI:10.3791/2356

15. Wu VCC, Takeuchi M, Otani K, et al (2013) Effect of through-plane and twisting motion on left ventricular strain calculation: Direct comparison between two-dimensional and three-dimensional speckle-tracking echocardiography. J Am Soc Echocardiogr. DOI:10.1016/j.echo.2013.07.006

16. Kowalik E, Kowalski M, Klisiewicz A, Hoffman P (2016) Global area strain is a sensitive marker of subendocardial damage in adults after optimal repair of aortic coarctation: three-dimensional speckle-tracking echocardiography data. Heart Vessels. DOI:10.1007/s00380-016-0803-4

17. Kleijn SA, Aly MFA, Terwee CB, Van Rossum AC, Kamp O (2011) Three-dimensional speckle tracking echocardiography for automatic assessment of global and regional left ventricular function based on area strain. J Am Soc Echocardiogr. DOI:10.1016/j.echo.2011.01.014

18. Ogawa A, Matsubara H (2015) Balloon Pulmonary Angioplasty: A Treatment Option for Inoperable Patients with Chronic Thromboembolic Pulmonary Hypertension. Front Cardiovasc Med. DOI:10.3389/fcvm.2015.00004

19. Lang IM, Madani M (2014) Update on chronic thromboembolic pulmonary hypertension. Circulation. DOI:10.1161/CIRCULATIONAHA.114.009309

20. Alfakih K, Plein S, Bloomer T, Jones T, Ridgway J, Sivananthan M (2003) Comparison of right ventricular volume measurements between axial and short axis orientation using steady-state free precession magnetic resonance imaging. J Magn Reson Imaging. DOI:10.1002/jmri.10329

21. Kawakubo M, Nagao M, Kumazawa S, et al (2016) Evaluation of ventricular dysfunction using semi-automatic longitudinal strain analysis of four-chamber cine MR imaging. Int J Cardiovasc Imaging. DOI:10.1007/s10554-015-0771-2

22. Jamieson SW, Auger WR, Fedullo PF, Channick RN, Kriett JM, Tarazi RY MK (1993) Experience and results with 150 pulmonary thromboendarterectomy operations over a 29-month period. J Thorac Cardiovasc Surg 106:126-127

23. Hayashi K, Tsuda T, Nomura A, Fujino N, Nohara A, Sakata K, Konno T, Nakanishi C, Tada H, Nagata Y, Teramoto R, Tanaka Y, Kawashiri MA YMH-PARI (2018) Impact of B-Type

Natriuretic Peptide Level on Risk Stratification of Thromboembolism and Death in Patients With Nonvalvular Atrial Fibrillation ― The Hokuriku-Plus AF Registry ―. Circ J. DOI:10.1253/circj.CJ-17-1085

24. Maceira AM, Prasad SK, Khan M, Pennell DJ (2006) Reference right ventricular systolic and diastolic function normalized to age, gender and body surface area from steady-state free precession cardiovascular magnetic resonance. Eur Heart J. DOI:10.1093/eurheartj/ehl336

25. Hosokawa K, Abe K, Oi K, Mukai Y, Hirooka Y, Sunagawa K (2015) Negative acute hemodynamic response to balloon pulmonary angioplasty does not predicate the long-term outcome in patients with chronic thromboembolic pulmonary hypertension. Int J Cardiol. DOI:10.1016/j.ijcard.2015.04.025

26. Mizoguchi H, Ogawa A, Munemasa M, Mikouchi H, Ito H, Matsubara H (2012) Refined balloon pulmonary angioplasty for inoperable patients with chronic thromboembolic pulmonary hypertension. Circ Cardiovasc Interv. DOI:10.1161/CIRCINTERVENTIONS.112.971077

27. Carluccio E, Biagioli P, Alunni G, et al (2018) Prognostic Value of Right Ventricular Dysfunction in Heart Failure With Reduced Ejection FractionCLINICAL PERSPECTIVE. Circ Cardiovasc Imaging. DOI:10.1161/CIRCIMAGING.117.006894

28. Lu KJ, Chen JXC, Profitis K, et al (2015) Right ventricular global longitudinal strain is an independent predictor of right ventricular function: A multimodality study of cardiac magnetic resonance imaging, real time three-dimensional echocardiography and speckle tracking echocardiography. Echocardiography. DOI:10.1111/echo.12783

29. Leather HA (2006) Longitudinal but not circumferential deformation reflects global contractile function in the right ventricle with open pericardium. AJP Hear Circ Physiol. DOI:10.1152/ajpheart.01211.2004

30. Jiang D, Niwa M, Koong AC, Diego S (2016) HHS Public Access. Eur J Vasc Endovasc Surg. DOI:10.1016/j.semcancer.2015.04.010.Targeting

31. López-Candales A, Edelman K, Candales MD (2010) Right ventricular apical contractility in

acute pulmonary embolism: The mcconnell sign revisited. Echocardiography. DOI:10.1111/j.1540-8175.2009.01103.x

32. Alfakih K, Plein S, Thiele H, Jones T, Ridgway JP, Sivananthan MU (2003) Normal human left and right ventricular dimensions for MRI as assessed by turbo gradient echo and steady-state free precession imaging sequences. J Magn Reson Imaging. DOI:10.1002/jmri.10262

33. Schmidt B, Dick A, Treutlein M, et al (2017) Intra- and inter-observer reproducibility of global and regional magnetic resonance feature tracking derived strain parameters of the left and right ventricle. Eur J Radiol. DOI:10.1016/j.ejrad.2017.01.025

34. van Kessel M, Seaton D, Chan J, et al (2017) Erratum to: Prognostic value of right ventricular free wall strain in pulmonary hypertension patients with pseudo-normalized tricuspid annular plane systolic excursion values. Int J Cardiovasc Imaging. DOI:10.1007/s10554-016-1025-7

35. Liu B, Dardeer AM, Moody WE, Edwards NC, Hudsmith LE, Steeds RP (2018) Normal values for myocardial deformation within the right heart measured by feature-tracking cardiovascular

magnetic resonance imaging. Int J Cardiol. DOI:10.1016/j.ijcard.2017.10.106

Table and Figure legends

Table 1

Baseline clinical characteristics and balloon pulmonary angioplasty procedure of the study population.

Data are presented as median and interquartile range (IQR, 25th - 75th percentile).

CTEPH, chronic thromboembolic pulmonary hypertension; WHO, world health organization; BPA, balloon pulmonary angioplasty

Table 2

Hemodynamic, laboratory data and cardiac MRI characteristics of the study population. Data are presented as median and interquartile range (IQR, 25th - 75th percentile) s. Statistically significant p values ($p<0.05$) are highlighted in bold.

BPA, balloon pulmonary angioplasty; Δ, changes after BPA; mPAP, mean pulmonary artery pressure; 6MWD, 6-minute walking distance; BNP, brain natriuretic peptide; RV, right ventricular; CMRI, cardiac magnetic resonance imaging; RVEDVi, right ventricular end-diastolic volume index; RVESVi, right

ventricular end-systolic volume index; RVEF, right ventricular ejection fraction; SVi, stroke volume index; CI, cardiac index; LVEDVi, left ventricular end-diastolic volume index; LVESVi, left ventricular end-systolic volume index; LVEF, left ventricular ejection fraction

Table 3

Comparison of strains in patients with chronic thromboembolic hypertension before and after balloon pulmonary angioplasty. Data are presented as median and interquartile range (IQR, 25th - 75th percentile). Statistically significant p values ($p<0.05$) are highlighted in bold.

BPA, balloon pulmonary angioplasty; RV, right ventricular; GAS, global area strain; AS_{base}, basal area strain; AS_{mid}, middle area strain; AS_{apex}, apical area strain; LS, longitudinal strain; CS, circumferential strain; RS, radial strain

Table 4

Comparing the performance for detection of improved patients after BPA.

mPAP, mean pulmonary artery pressure; BNP, brain natriuretic peptide; RVEF, right ventricular ejection fraction; AUC, area under the curve; GAS, global area strain; AS_{base}, basal area strain; AS_{mid}, middle area strain; AS_{apex}, apical area strain; FTMRI, feature-tracking MRI; LS, longitudinal strain; CS, circumferential strain; RS, radial strain

Table 5

Spearman's rank correlation coefficients (ρ) between changes in strain values and changes in clinical indices, between changes in strain values and changes in right ventricular volumetric parameters after balloon pulmonary angioplasty. The *p* value refers to the correlation analysis.

*$p < 0.05$; **$p < 0.01$; Δ, changes after balloon pulmonary angioplasty; GAS, global area strain; AS_{base}, basal area strain; AS_{mid}, middle area strain; AS_{apex}, apical area strain; LS, longitudinal strain; CS, circumferential strain; RS, radial strain; mPAP, mean pulmonary artery pressure; 6MWD, 6-minute walking distance; BNP, brain natriuretic peptide; RV, right ventricular; CMRI, cardiac magnetic resonance imaging; RVEDVi, right ventricular end-diastolic volume index; RVESVi, right ventricular end-systolic volume index; RVEF, right ventricular ejection fraction

Table 6

Intra- and inter-observer reproducibility of the strain analysis.

LOA, limit of agreement; SDD, standard deviation of the difference; ICC, intraclass correlation coefficient; CI, confidence interval; FTMRI, feature-tracking MRI; GAS, global area strain; AS_{base}, basal area strain; AS_{mid}, middle area strain; AS_{apex}, apical area strain; LS, longitudinal strain; CS, circumferential strain; RS, radial strain

Figure 1

Area strain analysis is based on manual segmentation of the right ventricular (RV) surface. A) On the short-axis cine image, the endocardial RV surface was manually delineated as lines for a cardiac cycle. B) The delineated lines were plotted on 3-dimensional (3D) coordinates. C) The endocardial area was calculated from the surface area of the delineated lines. D) The endocardial area was segmented into basal, middle, and apical regions. E) The area strain of the whole right ventricle was calculated as a percentage of the end-diastolic area relative to the difference between the area of end-diastole and each

cardiac phase.

Figure 2

Correlations between right ventricular ejection fraction (RVEF) and global area strain (GAS), longitudinal strain (LS), circumferential strain (CS), and radial strain (RS). GAS, LS, and RS were significantly correlated with RVEF. No significant correlation could be identified between CS and RVEF. These plots include strain values before and after balloon pulmonary angioplasty (BPA).

Clinical usefulness of right ventricular 3D area strain in the assessment of treatment effects of balloon pulmonary angioplasty in chronic thromboembolic pulmonary hypertension: Comparison with 2D feature-tracking MRI

Abstract (230 / 250 words)

Objectives

To evaluate the usefulness of right ventricular (RV) area strain analysis via cardiac MRI (CMRI) as a tool for assessing the treatment effects of balloon pulmonary angioplasty (BPA) in inoperable chronic thromboembolic pulmonary hypertension (CTEPH), RV area strain was compared to two-dimensional (2D) strain with feature-tracking MRI (FTMRI) before and after BPA.

Methods

We retrospectively analyzed 21 CTEPH patients who underwent BPA. End-systolic global area strain (GAS), longitudinal strain (LS), circumferential strain (CS), and radial strain (RS) were measured before and after BPA. Changes in GAS and RV ejection fraction (RVEF) values after BPA were defined as

ΔGAS and ΔRVEF. Receiver operating characteristic (ROC) analyses were performed to determine the optimal cutoff of the strain at after BPA for detection of improved patients with decreased mean pulmonary artery pressure (mPAP) less than 30 mmHg and increased RVEF more than 50 %.

Results

ROC analysis revealed the optimal cutoffs of strains (GAS, LS, CS, and RS) for identifying improved patients with mPAP<30 mmHg (cutoff (%) = -41.2, -13.8, -16.7, and 14.4: area under the curve, 0.75, 0.56, 0.65, and 0.75) and patients with RVEF>50 % (cutoff (%) = -37.2, -29.5, -2.9, and 14.4: area under the curve, 0.81, 0.60, 0.56, and 0.56).

Conclusions

Area strain analysis via CMRI may be a more useful tool for assessing the treatment effects of BPA in patients with CTEPH than 2D strains with FTMRI.

Keywords (3 to 5)

Myocardial Contraction, Balloon Angioplasty, Cine Magnetic Resonance Imaging, Pulmonary Heart Disease, Right Ventricle

Key points (1 to 3)

- Area strain values can detect improvement of right ventricular (RV) pressure and function after balloon pulmonary angioplasty (BPA) equally or more accurately than two-dimensional strains.
- Area strain analysis is a useful analytical method that reflects improvements in complex RV myocardial deformation by BPA.
- Area strain analysis is a robust method with reproducibility equivalent to that of 2D strain analysis.

Abbreviations

CTEPH: chronic thromboembolic pulmonary hypertension

BPA: balloon pulmonary angioplasty

RV: right ventricular

CMRI: cardiac magnetic resonance imaging

FTMRI: feature-tracking magnetic resonance imaging

2D: two-dimensional

3D: three-dimensional

RHC: right heart catheterization

mPAP: mean pulmonary artery pressure

SSFP: steady-state free precession

TR: repetition time

TE: echo time

LV: left ventricular

EDV: end-diastolic volume

ESV: end-systolic volume

EF: ejection fraction

SVi: stroke volume index

CI: cardiac index

LS: longitudinal strain

CS: circumferential strain

RS: radial strain

GAS: global area strain

AS_{base}: basal area strain

AS_{mid}: middle area strain

AS_{apex}: apical area strain

IQR: inter quartile range

PVR: pulmonary vascular resistance

6MWD: 6-minute walking distance

BNP: brain natriuretic peptide

ROC: receiver operating characteristic

ICC: intraclass correlation coefficient

TAPSE: tricuspid annular plane systolic excursion

IVS: interventricular septum

Introduction

Chronic thromboembolic pulmonary hypertension (CTEPH) is a fatal disease characterized by thrombotic occlusion or narrowing of the pulmonary arteries resulting in pulmonary hypertension, right-side heart failure, and death [1,2]. Balloon pulmonary angioplasty (BPA) is a promising option for inoperable patients with CTEPH [3]. Considering that clinical parameters of right ventricular (RV) function are associated with prognosis, RV reverse remodeling, pulmonary pressure overload, and interventricular dyssynchrony in patients with CTEPH [4–8], noninvasive evaluation of RV function is paramount to accurately assess the effects of treatment during repeated BPA sessions. Echocardiographic strain imaging, such as tissue Doppler imaging and speckle tracking, is widely used in clinical examination for the assessment of myocardial function [9]. However, the echocardiographic strain imaging of the right ventricle has historically been challenging due to its complex morphology, thin wall with coarse trabeculations, and anterior position within the chest.

Recent developments in cardiac MRI (CMRI) have enabled image-based assessment of RV

function, and CMRI is currently considered the reference standard [10]. Feature-tracking MRI (FTMRI) enables tracking of tissue voxel motion using only standard two-dimensional (2D) cine MRI and the evaluation of wall mechanics and strains without the need for acquisition of additional sequences [11–14]. However, a fixed 2D slice plane lacks visual information pertaining to original myocardial features that is yielded by frame-by-frame tracking analysis [15]. Therefore, three-dimensional (3D) image-based analysis has a theoretical advantage compared to 2D analysis. Global and regional area strain determined via echocardiography, which quantifies 3D changes in the endocardial surface area, have been reported as sensitive predictors of myocardial damage [16,17]. To the best of our knowledge, there is no report describing the analysis of RV area strain via CMRI for assessing the treatment effects of BPA in patients with CTEPH. In the present study, we measured changes in 3D area strain and 2D strain before and after BPA to investigate the extent to which area strain analysis may constitute a useful tool for assessing the treatment effects of BPA, when compared to 2D strains assessed by FTMRI. We also inspected correlations between the changes of strains and physiological indices and RV function.

Materials and methods

Study population

This retrospective observational study was approved by our institutional review board, and written informed consent was obtained from each patient. Twenty-one patients with CTEPH were enrolled in the study, and datasets derived between May 2012 and December 2017 were analyzed. Inclusion criteria were being older than 20 years and in a clinically stable state. Diagnosis of CTEPH and eligibility for BPA were determined according to previously reported procedures and criteria [18,19]. To exclude left-side heart disease and pulmonary disease, all patients received echocardiography and high resolution computed tomography. All BPAs were performed in the peripheral pulmonary arteries and multiple pulmonary arterial lesions were dilated in the same BPA session. All patients underwent the first right heart catheterization (RHC) within 1 month before the first BPA session. Post-operative hemodynamic measurements were assessed 1 and 6 months after the last BPA session. CMRIs were performed within 1

month before the first BPA session and within 1 month after the last BPA session, when the mean pulmonary artery pressure (mPAP) had decreased less than 30mmHg.

Cine MR imaging

CMRI was performed using a 3.0-T clinical scanner (Achieva 3.0 T Quasar Dual; Philips Healthcare), equipped with dual-source parallel radiofrequency transmission and a cardiac phased array 32-channel receiver coil. Cine steady-state free precession (SSFP) images were obtained using a multi-breath holding (approximately 10–20 s) SSFP sequence, with retrospective electrocardiogram gating in the 4-chamber view and in contiguous short-axis views covering the whole left ventricle and right ventricle with approximately 10 images and with 20 phases per cardiac cycle. The cine imaging parameters were repetition time (TR) 2.8 ms, echo time (TE) 1.4 ms, SENSE factor 2.0, flip angle 45°, slice thickness 8 mm, slice gap 0 mm, field of view 380 × 380 mm2, acquisition matrix 176 × 193, and reconstruction matrix 352 × 352. RV volume analysis was performed semi-automatically with subsequent manual correction using a workstation (IntelliSpace Portal, Philips Healthcare). RV volumes were measured on

the basis of axial images as previous report [20]. Left ventricular (LV) volumes were measured on the basis of short-axis images. End-diastolic volume (EDV) and end-systolic volume (ESV) were indexed to the body surface area, and these values were designated EDVi and ESVi. The ejection fraction (EF) was calculated via EDV and ESV. Stroke volume index (SVi) was calculated as the difference between EDVi and ESVi. Cardiac index (CI) was the product of SVi and heart rate.

Strain analysis using 2D cine MRI

Myocardial strain was analyzed semi-automatically with subsequent manual correction using an in-house original off-line feature-tracking tool that has been validated in a previous clinical study [21]. This algorithm was designed using MATLAB R2017b version 9.3 (The Mathworks Inc., Massachusetts). First, endocardial borders, including the ventricular septum, were manually defined as some arbitrary points at the end of diastole. The endocardium points were then tracked for a cardiac cycle with a local template-matching technique based on normalized correlation coefficient values. Lastly, the strain values for a cardiac cycle were automatically calculated from the coordinates of each point. End-systolic

longitudinal strain (LS), circumferential strain (CS), and radial strain (RS) were defined as the peak value of each strain. CS and RS analyses were performed based on short-axis cine imaging in the middle of the right ventricle, and LS analysis was performed via four-chamber cine imaging.

Area strain analysis with 2D cine MRI

Area strain analyses were conducted using MATLAB-based manual segmentation of the RV surface. On the short-axis cine image, the endocardial surface of the right ventricle, including ventricular septum, was manually delineated as lines for a cardiac cycle (Fig. 1A). The delineated lines were plotted on 3D coordinates (Fig. 1B). Endocardial area of the whole RV was calculated from these lines by spline interpolation for each time phase (Fig. 1C). The endocardial area was then segmented into basal, middle, and apical regions by dividing the ventricle cavity in three equal longitudinal length segments (Fig. 1D). These segmentations were performed for each time phase during one cardiac cycle. During RV contraction, the endocardial surface area decreases in size because of longitudinal and circumferential shortening and radial myocardial thickening [17]. Area strain reflects this change in the endocardial

surface area (Area(t)), and provides a quantitative metric representing the percentage change in area from its original dimensions (Area(D)), calculated as per below:

$$Area\ strain(\%) = \frac{Area(t) - Area(D)}{Area(D)} \times 100$$

The end-systolic global area strain (GAS) and basal, middle, and apical area strain (AS_{base}, AS_{mid}, and AS_{apex}) were the minimum peak area of each area strain (Fig. 1E).

Statistically analysis

The Shapiro-Wilk test was employed to assess normality of data distribution. Due to non-normal data distribution, descriptive statistics are provided as median and the corresponding inter quartile ranges (IQR). The area strain values GAS, AS_{base}, AS_{mid}, and AS_{apex} and the LS, CS, and RS values before and after BPA were compared using the Wilcoxon signed-rank test. Changes in strain values (GAS, AS_{base}, AS_{mid}, and AS_{apex}, as well as LS, CS, and RS), mPAP, pulmonary vascular resistance (PVR), 6-minute walking distance (6MWD), brain natriuretic peptide (BNP), RVEDVi, RVESVi, and RVEF before and after BPA were defined as ΔGAS, ΔAS_{base}, ΔAS_{mid}, ΔAS_{apex}, ΔLS, ΔCS, ΔRS, ΔmPAP, ΔPVR, Δ6MWD,

ΔBNP, ΔRVEDVi, ΔRVESVi, and ΔRVEF. Receiver operating characteristic (ROC) analyses were performed to determine the optimal cutoff of the strain for detection of improved patients after BPA, defined as: mPAP<30 mmHg [22], BNP<18.4 pg/mL [23], and RVEF>50 % [24]. The differences of ROCs of AS_{base}, AS_{mid}, and AS_{apex} were tested against each other by DeLong's test. Correlations between changes in strain values (ΔGAS, ΔAS_{base}, ΔAS_{mid}, ΔAS_{apex}, ΔLS, ΔCS, and ΔRS) and changes in clinical indices (ΔmPAP, ΔPVR, Δ6MWD, and ΔBNP) after BPA were calculated using Spearman's rank correlation coefficient (ρ). Similarly, ρ values were calculated between changes in strain values and changes in RV volumetric parameters (ΔRVEDVi, ΔRVESVi, and ΔRVEF). Correlations between strains (GAS, AS_{base}, AS_{mid}, and AS_{apex}, as well as LS, CS, and RS) and RVEF were calculated before and after BPA. All statistical analyses were conducted using the SAS software for Windows (version 13, SAS Inc.). Statistical significance was set at $p < 0.05$.

Intra- and inter-observer reproducibility

All 2D and 3D strain measurements were tested for intra-observer reproducibility by having one

observer performing all GAS analyses on 10 randomly selected patients, 5 in the before BPA group and 5 in the after BPA group, then blindly repeating the analyses on a separate occasion. Inter-observer reproducibility was evaluated by a second observer blinded to the clinical and experimental data, performing GAS measurements on the same 10 patients. Intra- and inter-observer reproducibility of the measurements of GAS, AS_{base}, AS_{mid}, AS_{apex}, CS, LS, and RS were evaluated using Bland-Altman analyses and intraclass correlation coefficient (ICC) with one-way random single measures or two-way random single measures (ICC(1, 1) or ICC(2,1)). ICCs were defined as excellent (ICC $\geq$ 0.75), good (ICC = 0.60 - 0.74), moderate (ICC = 0.40 - 0.59) and poor (ICC $\leq$ 0.39).

Results

Baseline clinical characteristics and BPA procedure are shown in Table 1. BPA procedures were successfully performed in all patients. Hemodynamic and laboratory data and CMRI characteristics of the study population are shown in Table 2. The clinical indices of mPAP, PVR, 6MWD, and BNP were

significantly improved after BPA. The RV functions RVEDVi, RVESVi, and RVEF as measured via CMRI were also significantly improved after BPA. The LV function was preserved and stable before and after BPA. Table 3 shows the 2D strains and area strains before and after BPA. GAS, AS_{base}, AS_{apex}, LS, and RS were significantly improved after BPA.

ROC analysis was used to describe the optimal cutoffs of 3D strains (GAS, AS_{base}, AS_{mid}, and AS_{apex}) and 2D strains (LS, CS, and RS) in order to identify improved patients with mPAP <30 mmHg, BNP <18.4 pg/mL, and RVEF >50% (shown in Table 4). There were significant differences only between the ROC curves of AS_{base} and AS_{apex} in all comparisons ($p = 0.02$). Spearman's rank correlations between changes in strain values and changes in clinical indices and between changes in strain values and changes in RV volumetric parameters after BPA are shown in Table 5. The ΔGAS was significantly correlated with ΔBNP, ΔRVESVi, and ΔRVEF ($\rho = 0.57$, 0.61, and -0.68; $p < 0.01$ for all tested correlations). The ΔAS_{mid} was significantly correlated with ΔRVEF ($\rho = -0.52$, $p < 0.05$). The ΔAS_{apex} was significantly correlated with ΔPVR, ΔBNP, ΔRVEDVi, and ΔRVESVi ($\rho = 0.65$, 0.44, 0.46,

and 0.56; $p < 0.01$, $p < 0.05$, $p < 0.05$, and $p < 0.01$). The ΔLS was significantly correlated with ΔRVESVi and ΔRVEF (ρ = 0.47 and -0.44; $p < 0.05$ for all tested correlations). The ΔRS was significantly correlated with ΔRVEDVi, ΔRVESVi, and ΔRVEF (ρ = -0.51, -0.55, and -0.54; $p < 0.05$ for all tested correlations). GAS, LS, and RS were significantly correlated with RVEF (ρ = -0.66, -0.44, and 0.58; $p < 0.01$ for all tested correlations). No significant correlation between CS and RVEF could be identified (ρ = -0.20, p = 0.19) (Fig. 2). AS_{base}, AS_{mid}, and AS_{apex} were significantly correlated with RVEF (ρ = -0.54, -0.33, and 0.58; $p < 0.01$, $p < 0.05$, and $p < 0.01$).

The intra- and inter-observer reproducibility for strain analyses are shown in Table 6. Excellent intra- and inter-observer reproducibility could be observed. Bland-Altman analysis indicated small bias and standard deviation of the difference and a narrow limit of agreement. All ICCs were indicative of excellent reproducibility (ICC>0.75, $p < 0.01$).

Discussion

The current study yielded three major findings. Firstly, area strain values can detect improvement of the RV pressure (mPAP) and function (RVEF) after BPA equally or more accurately than 2D strains, possibly constituting an improved tool for assessing treatment effects of BPA. Secondly, area strain analysis is a useful analytical method that reflects improvements in complex RV myocardial deformation by BPA. Lastly, area strain analysis is a robust method with reproducibility equivalent to that of 2D strain analysis.

In the present study, area strain and 2D strain were analyzed in patients with CTEPH before and after BPA, as clinical indicators of the treatment effects of BPA. Physiological examination parameters (mPAP, PVR, 6MWD, and BNP) and RV function determined via CMRI were significantly improved after BPA. Reflecting the decrease in HR and RV volumes, there were no significant differences in SVi or CI after BPA. In the patients of present study, the period of CMRI between before and after BPA was not uniformed. Because BPA does not immediately improve hemodynamics, and it takes several weeks to observe major effects [25]. Also the improved hemodynamics were maintained even 1year after BPA

[26]. One of the main goals of this study was to investigate the clinical usefulness of area strain analysis for assessing the treatment effects of BPA, given CMRI confirmation of patients who clearly improved after treatment. Nevertheless, further studies should also investigate how useful GAS can be as a quantitative tool assessing the treatment effects of BPA during repeated sessions. Our ROC analyses support good diagnostic performance of the GAS and 2D strains measured after BPA for detecting changes to normal in the case of the mPAP (<30mmHg), the BNP (<18.4pg/mL) and the RVEF (>50%). In the analyses of mPAP and RVEF, area strain values could detect their improvement after BPA equally or more accurately than 2D strains. However, low diagnostic performance was observed in all strains for the BNP analysis – indeed, only the ΔGAS was significantly correlated the ΔBNP. Altogether, these data suggest area strain analysis may constitute an useful tool for assessing treatment effects of BPA. In the comparison of the ROC curves of 3D regional area strains (AS_{base}, AS_{mid}, and AS_{apex}), AS_{base} detected only normal change in mPAP, but the detectability in other comparisons was equivalent. In contrast, ΔAS_{apex} was significantly correlated with ΔPVR, ΔBNP, ΔRVEDVi, and ΔRVESVi. Based on these

results, we concluded that AS_{apex} is a more useful marker to assess the treatment effects of BPA.

GAS was significantly improved after BPA and correlated significantly with RVEF. It has been previously reported that LS is a sensitive marker for the evaluation of RV function [27,28]. In the present study, LS also significantly improved after BPA and correlated significantly with RVEF. There was no significant difference in the CS before and after BPA. However, sight should not be lost that previous studies have reported that the right ventricle, having a two-layer muscular fiber, deforms largely on the long axis [29] and that RV myocardium not only contracts but twists [30]. Both of these are motions towards the center of the heart, which is the middle of the ventricle. Thus, in the RV that moves largely in the long axis direction, the motion to the ventricular middle is less than to the ventricle base and apex. Considering that the CS was measured at the middle ventricular level, the motion peculiarities may underlie this result. However, we acknowledge that further investigation is needed to support or reject this hypothesis. Furthermore, an advantage of area strain with regard to RVEF is the quantification of regional myocardial deformation. In patients with CTEPH, AS_{base} and AS_{apex}

significantly improve after BPA, but AS_{mid} does not. These results are consistent with those presented by López-Candales et al.'s [31], where the authors reported on the progressive reduction in the basal and apical RV strain during chronic pulmonary hypertension. In addition to the CS, also the results of AS_{mid} may be due to the basic characteristics of the RV motion mechanism. Area strain analysis may, thus, be a useful analytical method reflecting improvements in complex RV myocardial deformation after BPA.

Importantly, we found both 3D and 2D strain analyses to exhibit excellent reproducibility in our intra- and inter-observer analysis. The reproducibility of 2D strain, as assessed via FTMRI, had been previously validated[32,33]. Therefore, we consider that area strain analysis is a robust method with equivalent reproducibility to 2D strain analysis via FTMRI. We also know that the tricuspid annular plane systolic excursion (TAPSE), evaluated through echocardiography, is a common and easy tool to assess RV function. However, the superiority of RV longitudinal strain over TAPSE had been previously reported [27,34]. These were analyses of strains of RV free walls only. In our study we aimed to move a step forward by including strains of the interventricular septum (IVS) in all analyses. Nevertheless, one

should note that the inclusion of IVS into RV mechanical analysis is a subject of intense debate. It is not clear whether free-wall and septum or only free-wall measures may be more useful as a marker of RV contractility [10,35]. It is a possible scenario that the difference between these two measurements is mostly technical. On the other hands, pulmonary hypertension is associated with a RV contraction delay. Loss of a coordinated ventricular contraction results in impaired RV systolic function. The prolonged RV contraction during early LV diastole causes the already relaxing interventricular septum to bulge into the LV. This negatively influences early LV filling, and eventually contributes to reduction of stroke volume [7]. Therefore, it seems likely that IVS may play an important role in assessment of RV function at least during pulmonary hypertension. We also note that with our method, myocardial area strain can be derived from routine MRI without additional image acquisition. This feature, along with its excellent reproducibility, strongly supports the feasibility and cost-effectiveness of our approach to be used in the clinical routine.

Limitations

Some limitations should be acknowledged. Area strain was not compared with other 3D strain parameters. The reason for this was that 3D strain analysis of RV has not been sufficiently established, and 2D evaluation is still mainstream. Although only the global 2D strains could be evaluated due to the specifications of our in-house software, area strain was compared with RV volumetric functions and strain, as determined via CMRI. Further studies should compare regional area and regional 2D strains in order to provide a more detailed picture. Another major limitation of this research is our small sample size (n = 21) and the absence of a control group. In addition to low sensitivity and specificity, there was a lack of significant differences in comparisons of AUC in ROC analyses. We suspect that these results caused the small number of patients and influenced the patient background in this study. Patients after BPA were enrolled at the endpoint of treatment (mPAP <30 mmHg). The large difference between patients with and without improved strains is a bias in the ROC analysis. We believe our approach, although promising, cannot be moved forward before evidence from further analyses with large cohorts and inclusion of controls might be gathered.

Conclusions

Area strain analysis may be a robust and useful tool for assessing the treatment effects of BPA. Once further confirmatory evidence might be gathered, this approach is likely to constitute an improved and cost-effective tool potentially useful for the clinical examination of patients with CTEPH.

Acknowledgements

This work was supported by JSPS KAKENHI Grant Number JP16K19860 and by Kyushu University Research Activity Support Program Foreign language Proofreading Expenses Support.

References

1. Pepke-Zaba J, Delcroix M, Lang I, et al (2011) Chronic thromboembolic pulmonary hypertension (CTEPH): Results from an international prospective registry. Circulation. DOI:10.1161/CIRCULATIONAHA.110.015008

2. Moneta GL(2006) Incidence of Chronic Thromboembolic Pulmonary Hypertension After Pulmonary Embolism. Yearb Vasc Surg. DOI:10.1016/S0749-4041(08)70317-8

3. Feinstein JA, Goldhaber SZ, Lock JE, Ferndandes SM, Landzberg MJ (2001) Balloon Pulmonary Angioplasty for Treatment of Chronic Thromboembolic Pulmonary Hypertension. Circulation. DOI:10.1161/01.CIR.103.1.10

4. Fukui S, Ogo T, Morita Y, et al (2014) Right ventricular reverse remodelling after balloon pulmonary angioplasty. Eur Respir J. DOI:10.1183/09031936.00012914

5. Kamimura Y, Okumura N, Adachi S, et al (2018) Usefulness of scoring right ventricular function for assessment of prognostic factors in patients with chronic thromboembolic pulmonary

hypertension. Heart Vessels. DOI:10.1007/s00380-018-1168-7

6. Rolf A, Rixe J, Kim WK, et al (2014) Right ventricular adaptation to pulmonary pressure load in patients with chronic thromboembolic pulmonary hypertension before and after successful pulmonary endarterectomy--a cardiovascular magnetic resonance study. J Cardiovasc Magn Reson. DOI:10.1186/s12968-014-0096-7

7. Yamasaki Y, Nagao M, Abe K, et al (2017) Balloon pulmonary angioplasty improves interventricular dyssynchrony in patients with inoperable chronic thromboembolic pulmonary hypertension: a cardiac MR imaging study. Int J Cardiovasc Imaging. DOI:10.1007/s10554-016-0985-y

8. Surie S, Reesink HJ, Marcus JT, et al (2013) Bosentan treatment is associated with improvement of right ventricular function and remodeling in chronic thromboembolic pulmonary hypertension. Clin Cardiol. DOI:10.1002/clc.22197

9. Gorcsan J, Tanaka H. Echocardiographic assessment of myocardial strain (2011) J Am Coll

Cardiol. DOI:10.1016/j.jacc.2011.06.038

10. Prati G, Vitrella G, Allocca G, et al (2015) Right Ventricular Strain and Dyssynchrony Assessment in Arrhythmogenic Right Ventricular Cardiomyopathy: Cardiac Magnetic Resonance Feature-Tracking Study. Circ Cardiovasc Imaging. DOI:10.1161/CIRCIMAGING.115.003647

11. Pedrizzetti G, Claus P, Kilner PJ, Nagel E (2016) Principles of cardiovascular magnetic resonance feature tracking and echocardiographic speckle tracking for informed clinical use. J Cardiovasc Magn Reson. DOI:10.1186/s12968-016-0269-7

12. Nagao M, Yamasaki Y (2018) Cardiac Strain Analysis Using Cine Magnetic Resonance Imaging and Computed Tomography. Cardiovasc Imaging Asia. DOI:10.22468/cvia.2018.00052

13. Schuster A, Hor KN, Kowallick JT, Beerbaum P, Kutty S (2016) Cardiovascular Magnetic Resonance Myocardial Feature Tracking: Concepts and Clinical Applications. Circ Cardiovasc Imaging. DOI:10.1161/CIRCIMAGING.115.004077

14. Hor KN, Baumann R, Pedrizzetti G, et al (2011) Magnetic Resonance Derived Myocardial Strain

Assessment Using Feature Tracking. J Vis Exp. DOI:10.3791/2356

15. Wu VCC, Takeuchi M, Otani K, et al (2013) Effect of through-plane and twisting motion on left ventricular strain calculation: Direct comparison between two-dimensional and three-dimensional speckle-tracking echocardiography. J Am Soc Echocardiogr. DOI:10.1016/j.echo.2013.07.006

16. Kowalik E, Kowalski M, Klisiewicz A, Hoffman P (2016) Global area strain is a sensitive marker of subendocardial damage in adults after optimal repair of aortic coarctation: three-dimensional speckle-tracking echocardiography data. Heart Vessels. DOI:10.1007/s00380-016-0803-4

17. Kleijn SA, Aly MFA, Terwee CB, Van Rossum AC, Kamp O (2011) Three-dimensional speckle tracking echocardiography for automatic assessment of global and regional left ventricular function based on area strain. J Am Soc Echocardiogr. DOI:10.1016/j.echo.2011.01.014

18. Ogawa A, Matsubara H (2015) Balloon Pulmonary Angioplasty: A Treatment Option for Inoperable Patients with Chronic Thromboembolic Pulmonary Hypertension. Front Cardiovasc Med. DOI:10.3389/fcvm.2015.00004

19. Lang IM, Madani M (2014) Update on chronic thromboembolic pulmonary hypertension. Circulation. DOI:10.1161/CIRCULATIONAHA.114.009309

20. Alfakih K, Plein S, Bloomer T, Jones T, Ridgway J, Sivananthan M (2003) Comparison of right ventricular volume measurements between axial and short axis orientation using steady-state free precession magnetic resonance imaging. J Magn Reson Imaging. DOI:10.1002/jmri.10329

21. Kawakubo M, Nagao M, Kumazawa S, et al (2016) Evaluation of ventricular dysfunction using semi-automatic longitudinal strain analysis of four-chamber cine MR imaging. Int J Cardiovasc Imaging. DOI:10.1007/s10554-015-0771-2

22. Jamieson SW, Auger WR, Fedullo PF, Channick RN, Kriett JM, Tarazi RY MK (1993) Experience and results with 150 pulmonary thromboendarterectomy operations over a 29-month period. J Thorac Cardiovasc Surg 106:126-127

23. Hayashi K, Tsuda T, Nomura A, Fujino N, Nohara A, Sakata K, Konno T, Nakanishi C, Tada H, Nagata Y, Teramoto R, Tanaka Y, Kawashiri MA YMH-PARI (2018) Impact of B-Type

Natriuretic Peptide Level on Risk Stratification of Thromboembolism and Death in Patients With Nonvalvular Atrial Fibrillation ― The Hokuriku-Plus AF Registry ―. Circ J. DOI:10.1253/circj.CJ-17-1085

24. Maceira AM, Prasad SK, Khan M, Pennell DJ (2006) Reference right ventricular systolic and diastolic function normalized to age, gender and body surface area from steady-state free precession cardiovascular magnetic resonance. Eur Heart J. DOI:10.1093/eurheartj/ehl336

25. Hosokawa K, Abe K, Oi K, Mukai Y, Hirooka Y, Sunagawa K (2015) Negative acute hemodynamic response to balloon pulmonary angioplasty does not predicate the long-term outcome in patients with chronic thromboembolic pulmonary hypertension. Int J Cardiol. DOI:10.1016/j.ijcard.2015.04.025

26. Mizoguchi H, Ogawa A, Munemasa M, Mikouchi H, Ito H, Matsubara H (2012) Refined balloon pulmonary angioplasty for inoperable patients with chronic thromboembolic pulmonary hypertension. Circ Cardiovasc Interv. DOI:10.1161/CIRCINTERVENTIONS.112.971077

27. Carluccio E, Biagioli P, Alunni G, et al (2018) Prognostic Value of Right Ventricular Dysfunction in Heart Failure With Reduced Ejection FractionCLINICAL PERSPECTIVE. Circ Cardiovasc Imaging. DOI:10.1161/CIRCIMAGING.117.006894

28. Lu KJ, Chen JXC, Profitis K, et al (2015) Right ventricular global longitudinal strain is an independent predictor of right ventricular function: A multimodality study of cardiac magnetic resonance imaging, real time three-dimensional echocardiography and speckle tracking echocardiography. Echocardiography. DOI:10.1111/echo.12783

29. Leather HA (2006) Longitudinal but not circumferential deformation reflects global contractile function in the right ventricle with open pericardium. AJP Hear Circ Physiol. DOI:10.1152/ajpheart.01211.2004

30. Jiang D, Niwa M, Koong AC, Diego S (2016) HHS Public Access. Eur J Vasc Endovasc Surg. DOI:10.1016/j.semcancer.2015.04.010.Targeting

31. López-Candales A, Edelman K, Candales MD (2010) Right ventricular apical contractility in

acute pulmonary embolism: The mcconnell sign revisited. Echocardiography. DOI:10.1111/j.1540-8175.2009.01103.x

32. Alfakih K, Plein S, Thiele H, Jones T, Ridgway JP, Sivananthan MU (2003) Normal human left and right ventricular dimensions for MRI as assessed by turbo gradient echo and steady-state free precession imaging sequences. J Magn Reson Imaging. DOI:10.1002/jmri.10262

33. Schmidt B, Dick A, Treutlein M, et al (2017) Intra- and inter-observer reproducibility of global and regional magnetic resonance feature tracking derived strain parameters of the left and right ventricle. Eur J Radiol. DOI:10.1016/j.ejrad.2017.01.025

34. van Kessel M, Seaton D, Chan J, et al (2017) Erratum to: Prognostic value of right ventricular free wall strain in pulmonary hypertension patients with pseudo-normalized tricuspid annular plane systolic excursion values. Int J Cardiovasc Imaging. DOI:10.1007/s10554-016-1025-7

35. Liu B, Dardeer AM, Moody WE, Edwards NC, Hudsmith LE, Steeds RP (2018) Normal values for myocardial deformation within the right heart measured by feature-tracking cardiovascular

magnetic resonance imaging. Int J Cardiol. DOI:10.1016/j.ijcard.2017.10.106

Table and Figure legends

Table 1

Baseline clinical characteristics and balloon pulmonary angioplasty procedure of the study population.

Data are presented as median and interquartile range (IQR, 25th - 75th percentile).

CTEPH, chronic thromboembolic pulmonary hypertension; WHO, world health organization; BPA, balloon pulmonary angioplasty

Table 2

Hemodynamic, laboratory data and cardiac MRI characteristics of the study population. Data are presented as median and interquartile range (IQR, 25th - 75th percentile) s. Statistically significant p values ($p<0.05$) are highlighted in bold.

BPA, balloon pulmonary angioplasty; Δ, changes after BPA; mPAP, mean pulmonary artery pressure; 6MWD, 6-minute walking distance; BNP, brain natriuretic peptide; RV, right ventricular; CMRI, cardiac magnetic resonance imaging; RVEDVi, right ventricular end-diastolic volume index; RVESVi, right

ventricular end-systolic volume index; RVEF, right ventricular ejection fraction; SVi, stroke volume index; CI, cardiac index; LVEDVi, left ventricular end-diastolic volume index; LVESVi, left ventricular end-systolic volume index; LVEF, left ventricular ejection fraction

Table 3

Comparison of strains in patients with chronic thromboembolic hypertension before and after balloon pulmonary angioplasty. Data are presented as median and interquartile range (IQR, 25th - 75th percentile). Statistically significant p values ($p<0.05$) are highlighted in bold.

BPA, balloon pulmonary angioplasty; RV, right ventricular; GAS, global area strain; AS_{base}, basal area strain; AS_{mid}, middle area strain; AS_{apex}, apical area strain; LS, longitudinal strain; CS, circumferential strain; RS, radial strain

Table 4

Comparing the performance for detection of improved patients after BPA.

mPAP, mean pulmonary artery pressure; BNP, brain natriuretic peptide; RVEF, right ventricular ejection fraction; AUC, area under the curve; GAS, global area strain; AS_{base}, basal area strain; AS_{mid}, middle area strain; AS_{apex}, apical area strain; FTMRI, feature-tracking MRI; LS, longitudinal strain; CS, circumferential strain; RS, radial strain

Table 5

Spearman's rank correlation coefficients (ρ) between changes in strain values and changes in clinical indices, between changes in strain values and changes in right ventricular volumetric parameters after balloon pulmonary angioplasty. The *p* value refers to the correlation analysis.

*$p < 0.05$; **$p < 0.01$; Δ, changes after balloon pulmonary angioplasty; GAS, global area strain; AS_{base}, basal area strain; AS_{mid}, middle area strain; AS_{apex}, apical area strain; LS, longitudinal strain; CS, circumferential strain; RS, radial strain; mPAP, mean pulmonary artery pressure; 6MWD, 6-minute walking distance; BNP, brain natriuretic peptide; RV, right ventricular; CMRI, cardiac magnetic resonance imaging; RVEDVi, right ventricular end-diastolic volume index; RVESVi, right ventricular end-systolic volume index; RVEF, right ventricular ejection fraction

Table 6

Intra- and inter-observer reproducibility of the strain analysis.

LOA, limit of agreement; SDD, standard deviation of the difference; ICC, intraclass correlation coefficient; CI, confidence interval; FTMRI, feature-tracking MRI; GAS, global area strain; AS_{base}, basal area strain; AS_{mid}, middle area strain; AS_{apex}, apical area strain; LS, longitudinal strain; CS, circumferential strain; RS, radial strain

Figure 1

Area strain analysis is based on manual segmentation of the right ventricular (RV) surface. A) On the short-axis cine image, the endocardial RV surface was manually delineated as lines for a cardiac cycle. B) The delineated lines were plotted on 3-dimensional (3D) coordinates. C) The endocardial area was calculated from the surface area of the delineated lines. D) The endocardial area was segmented into basal, middle, and apical regions. E) The area strain of the whole right ventricle was calculated as a percentage of the end-diastolic area relative to the difference between the area of end-diastole and each

cardiac phase.

Figure 2

Correlations between right ventricular ejection fraction (RVEF) and global area strain (GAS), longitudinal strain (LS), circumferential strain (CS), and radial strain (RS). GAS, LS, and RS were significantly correlated with RVEF. No significant correlation could be identified between CS and RVEF. These plots include strain values before and after balloon pulmonary angioplasty (BPA).

Table 1

Baseline clinical characteristics and balloon pulmonary angioplasty procedure of the study population. Data are presented as median and interquartile range (IQR, 25th - 75th percentile).

Patients with CTEPH (n = 21)	
Age (y)	64 (53 - 71)
Male/Female	3 / 18
Body surface area (m^2)	1.5 (1.4 - 1.6)
WHO classification	
Ⅱ	2
Ⅲ	18
Ⅳ	1
Medication	
Endothelin receptor antagonist	10
Oral prostacyclin analogue	8
Phosphodiesterase type-5 inhibitor	11
Soluble guanylate cyclase stimulator	9
BPA procedure	
Right lesions	8 (7 - 9)
Left lesions	6 (3 - 8)
Sessions	4 (3 - 5)
Period of CMRIs (month)	11 (6 - 19)

CTEPH, chronic thromboembolic pulmonary hypertension; WHO, world health organization; BPA, balloon pulmonary angioplasty

Table 2

Hemodynamic, laboratory data and cardiac MRI characteristics of the study population. Data are presented as median and interquartile range (IQR, 25th - 75th percentile) s. Statistically significant p values ($p<0.05$) are highlighted in bold.

	Before BPA (n = 21)	After BPA (n = 21)	*Δ*	*p* value
Hemodynamic and laboratory data				
Hear rate (beats/min)	73 (59 - 80)	63 (58 - 71)	-8 (-12 - 4)	**0.01**
mPAP (mmHg)	35 (30 - 48)	26 (24 - 29)	-9 (-18 - -6)	**0.0001**
PVR (Wood Unit)	6.5 (5.4 - 8.4)	3.9 (3.6 - 4.7)	-2.4 (-4.2 - -1.7)	**0.0001**
6MWD (m)	375 (330 - 410)	431 (400 - 475)	50 (25 - 80)	**0.005**
BNP (pg/mL)	36.2 (21.1 - 49.4)	15.8 (8.3 - 24.3)	-10.0 (-33.3 - -3.4)	**0.0002**
RV function with CMRI				
RVEDVi (mL/m^2)	112 (81 - 129)	92 (82 - 116)	-15 (-25 - 1)	**0.006**
RVESVi (mL/m^2)	67 (42 - 98)	54 (41 - 61)	-11 (-24 - -3)	**0.0005**
RVEF (%)	39 (31 - 50)	46 (41 - 48)	8 (1 - 11)	**0.009**
SVi (mL/m^2)	39 (33 - 45)	41 (37 - 45)	4 (0 - 8)	0.099
CI (L/min/m^2)	2.6 (2.3 - 3.3)	2.7 (2.2 - 3.0)	0.0 (-0.5 - 0.3)	0.69
LV function with CMRI				
LVEDVi (mL/m^2)	67 (61 - 76)	76 (67 - 81)	6 (1 - 12)	**0.04**
LVESVi (mL/m^2)	27 (24 - 36)	33 (24 - 35)	2 (-3 - 6)	0.45
LVEF (%)	57 (53 - 63)	57 (51 - 62)	0 (-3 - 6)	0.23
SVi (mL/m^2)	39 (33 - 43)	43 (40 - 47)	6 (1 - 9)	**0.04**
CI (L/min/m^2)	3.9 (2.5 - 5.7)	3.2 (2.6 - 4.4)	-0.3 (-1.5 - 0.2)	0.15

BPA, balloon pulmonary angioplasty; Δ, changes after BPA; mPAP, mean pulmonary artery pressure; 6MWD, 6-minute walking distance; BNP, brain natriuretic peptide; RV, right ventricular; CMRI, cardiac magnetic resonance imaging; RVEDVi, right ventricular end-diastolic volume index; RVESVi, right ventricular end-systolic volume index; RVEF, right ventricular ejection fraction; SVi, stroke volume index; CI, cardiac index; LVEDVi, left ventricular end-diastolic volume index; LVESVi, left ventricular end-systolic volume index; LVEF, left ventricular ejection fraction

Table 3

Comparison of strains in patients with chronic thromboembolic hypertension before and after balloon pulmonary angioplasty. Data are presented as median and interquartile range (IQR, 25th - 75th percentile). Statistically significant p values ($p<0.05$) are highlighted in bold.

	Before BPA	After BPA	*Δ*	*p* value
RV area strains (%)				
GAS	-23.5 (-27.0 - -14.7)	-34.9 (-27.0 - -14.7)	-13.7 (-16.6 - -5.4)	**0.0002**
AS_{base}	-23.3 (-28.6 - -14.0)	-31.8 (-35.4 - -26.1)	-9.9 (-12.1 - -1.6)	**0.001**
AS_{mid}	-29.3 (-41.7 - -21.4)	-33.4 (-38.4 - -30.3)	-1.0 (-10.5 - 6.1)	0.23
AS_{apex}	-25.2 (-30.2 - -5.4)	-40.8 (-45.0 - -25.9)	-19.1 (-34.0 - -8.5)	**0.0003**
RV 2D strains (%)				
LS	-16.5 (-22.0 - -13.4)	-22.9 (-25.7 - -19.7)	-2.6 (-12.2 - -1.3)	**0.003**
CS	-8.9 (-11.2 - -7.7)	-9.4 (-14.1 - -8.5)	-1.1 (-3.7 - -1.6)	0.20
RS	6.6 (3.5 - 9.2)	9.4 (7.8 - 11.5)	2.4 (0.0 - 4.9)	**0.005**

BPA, balloon pulmonary angioplasty; RV, right ventricular; GAS, global area strain; AS_{base}, basal area strain; AS_{mid}, middle area strain; AS_{apex}, apical area strain; LS, longitudinal strain; CS, circumferential strain; RS, radial strain

Table 4

Comparing the performance for detection of improved patients after BPA

	mPAP<30 mmHG				BNP<18.4 pg/mL				RVRF>50 %			
	Cutoff (%)	AUC	Sensitivity	Specificity	Cutoff (%)	AUC	Sensitivity	Specificity	Cutoff (%)	AUC	Sensitivity	Specificity
Area strain												
GAS	-41.2	0.75	0.20	1.00	-37.5	0.53	1.00	0.33	-37.2	0.81	0.88	0.75
AS_{base}	-46.3	0.84	0.20	1.00	-31.8	0.75	0.78	0.67	-42.8	0.81	1.00	0.25
AS_{mid}	-45.3	0.74	0.20	1.00	-33.2	0.65	0.67	0.67	-45.3	0.66	1.00	0.00
AS_{apex}	-51.8	0.45	0.00	1.00	-42.1	0.63	0.67	0.75	-51.8	0.65	1.00	0.00
FT-MRI												
LS	-13.8	0.56	0.00	1.00	-21.7	0.55	0.56	0.67	-29.5	0.60	1.00	0.00
CS	-16.7	0.65	0.20	1.00	-14.4	0.53	0.33	0.83	-2.9	0.56	1.00	0.00
RS	14.4	0.75	0.00	1.00	12.7	0.51	1.00	0.33	14.4	0.56	1.00	0.00

mPAP, mean pulmonary artery pressure; BNP, brain natriuretic peptide; RVEF, right ventricular ejection fraction; AUC, area under the curve; GAS, global area strain; AS_{base}, basal area strain; AS_{mid}, middle area strain; AS_{apex}, apical area strain; FTMRI, feature-tracking MRI; LS, longitudinal strain; CS, circumferential strain; RS, radial strain

Table 5

Spearman's rank correlation coefficients (ρ) between changes in strain values and changes in clinical indices, between changes in strain values and changes in right ventricular volumetric parameters after balloon pulmonary angioplasty. The *p* value refers to the correlation analysis.

	ΔGAS	ΔAS_{base}	ΔAS_{mid}	ΔAS_{apex}	ΔLS	ΔCS	ΔRS
Clinical indices							
ΔmPAP (mmHg)	0.28	-0.16	0.16	0.31	0.28	0.15	-0.09
ΔPVR (Wood Unit)	0.27	-0.29	0.04	0.65**	0.30	0.17	-0.30
Δ6MWD (m)	-0.27	-0.05	-0.28	0.06	-0.17	-0.08	0.14
ΔBNP (pg/mL)	0.57**	0.21	0.21	0.44*	0.20	0.12	-0.33
RV function with CMRI							
ΔRVEDVi (mL/m^2)	0.39	0.06	0.01	0.46*	0.44	0.42	-0.51*
ΔRVESVi (mL/m^2)	0.61**	0.13	0.26	0.56**	0.47*	0.37	-0.55*
ΔRVEF (%)	-0.68**	-0.14	-0.52*	-0.42	-0.44*	-0.20	0.54*

*$p < 0.05$; **$p < 0.01$; Δ, changes after balloon pulmonary angioplasty; GAS, global area strain; AS_{base}, basal area strain; AS_{mid}, middle area strain; AS_{apex}, apical area strain; LS, longitudinal strain; CS, circumferential strain; RS, radial strain; mPAP, mean pulmonary artery pressure; 6MWD, 6-minute walking distance; BNP, brain natriuretic peptide; RV, right ventricular; CMRI, cardiac magnetic resonance imaging; RVEDVi, right ventricular end-diastolic volume index; RVESVi, right ventricular end-systolic volume index; RVEF, right ventricular ejection fraction

Table 6

Intra- and inter-observer reproducibility of strain analysis.

	Intra-observer reproducibility			Inter-observer reproducibility		
Parameter	Bias (LOA)	SDD	ICC (95% CI)	Bias (LOA)	SDD	ICC (95% CI)
Area strain						
GAS	1.39 (-4.1-6.9)	2.8	0.94 (0.78-0.98)	2.28 (-2.8-7.4)	2.6	0.94 (0.80-0.99)
AS_{base}	0.33 (-2.4-3.0)	1.4	0.97 (0.89-0.99)	0.67 (-1.8-3.1)	1.3	0.97 (0.88-0.99)
AS_{mid}	3.23 (-7.8-14.2)	5.6	0.90 (0.67-0.97)	4.43 (-6.6-15.5)	5.6	0.91 (0.67-0.98)
AS_{apex}	0.43 (-5.7-6.6)	3.1	0.93 (0.76-0.98)	1.60 (-4.2-7.4)	2.9	0.92 (0.73-0.98)
FTMRI						
LS	-0.0071 (-3.5-3.5)	1.8	0.91 (0.70-0.98)	-0.56 (-3.7-2.5)	1.6	0.91 (0.67-0.98)
CS	0.98 (-3.0-5.0)	2.0	0.90 (0.68-0.97)	0.10 (-3.1-3.2)	1.6	0.95 (0.81-0.99)
RS	-0.56 (-4.6-3.4)	2.0	0.92 (0.73-0.98)	0.56 (-3.4-4.6)	2.0	0.91 (0.69-0.98)

LOA, limit of agreement; SDD, standard deviation of the difference; ICC, intraclass correlation coefficient; CI, confidence interval; FTMRI, feature-tracking MRI; GAS, global area strain; AS_{base}, basal area strain; AS_{mid}, middle area strain; AS_{apex}, apical area strain; LS, longitudinal strain; CS, circumferential strain; RS, radial strain

Figure
Click here to access/download;Figure;Figures.pdf

Fig. 1

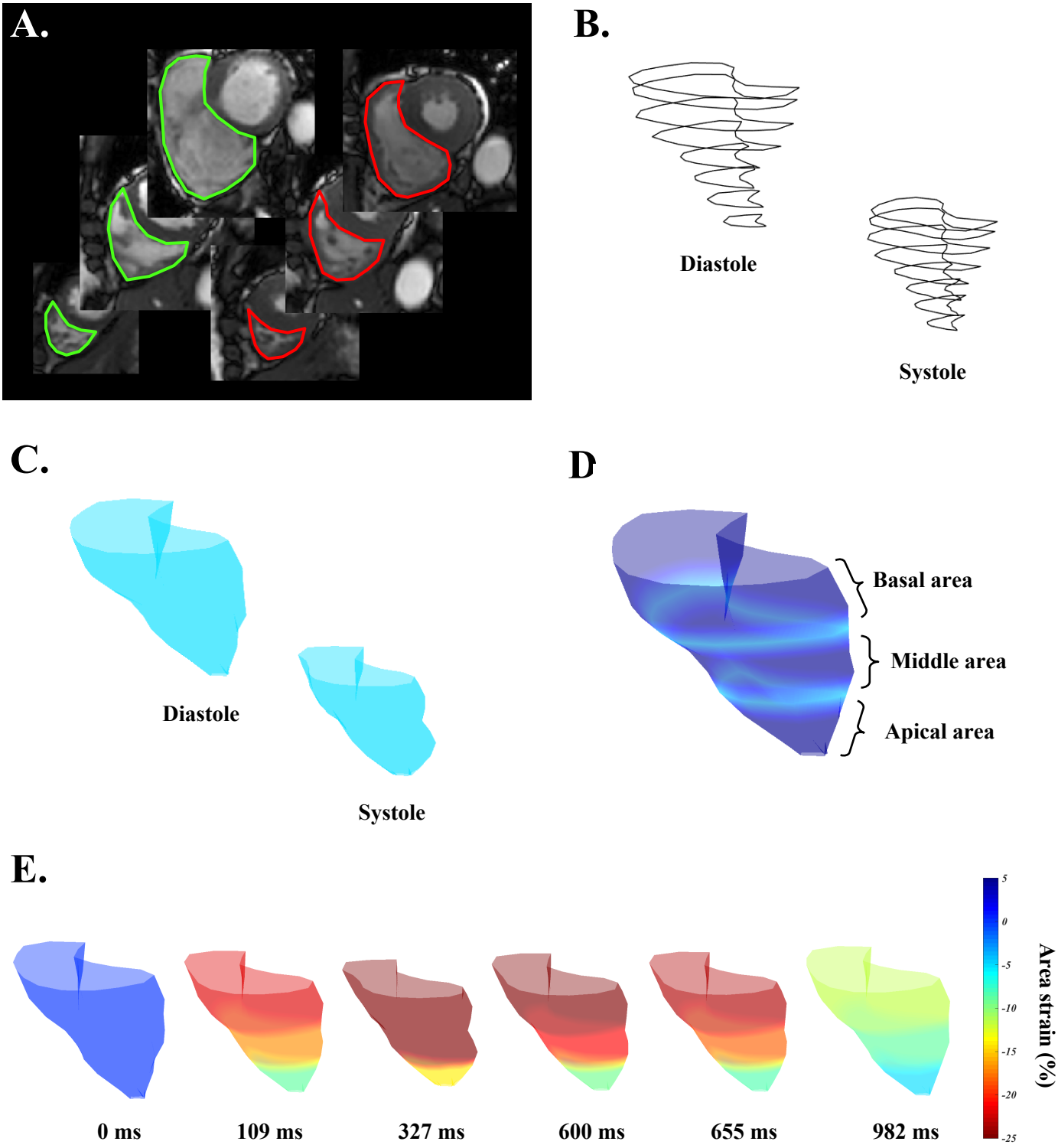

Area strain analysis is based on manual segmentation of the right ventricular (RV) surface. A) On the short-axis cine image, the endocardial RV surface was manually delineated as lines for a cardiac cycle. B) The delineated lines were plotted on 3-dimensional (3D) coordinates. C) The endocardial area was calculated from the surface area of the delineated lines. D) The endocardial area was segmented into basal, middle, and apical regions. E) The area strain of the whole right ventricle was calculated as a percentage of the end-diastolic area relative to the difference between the area of end-diastole and each cardiac phase.

Fig. 2

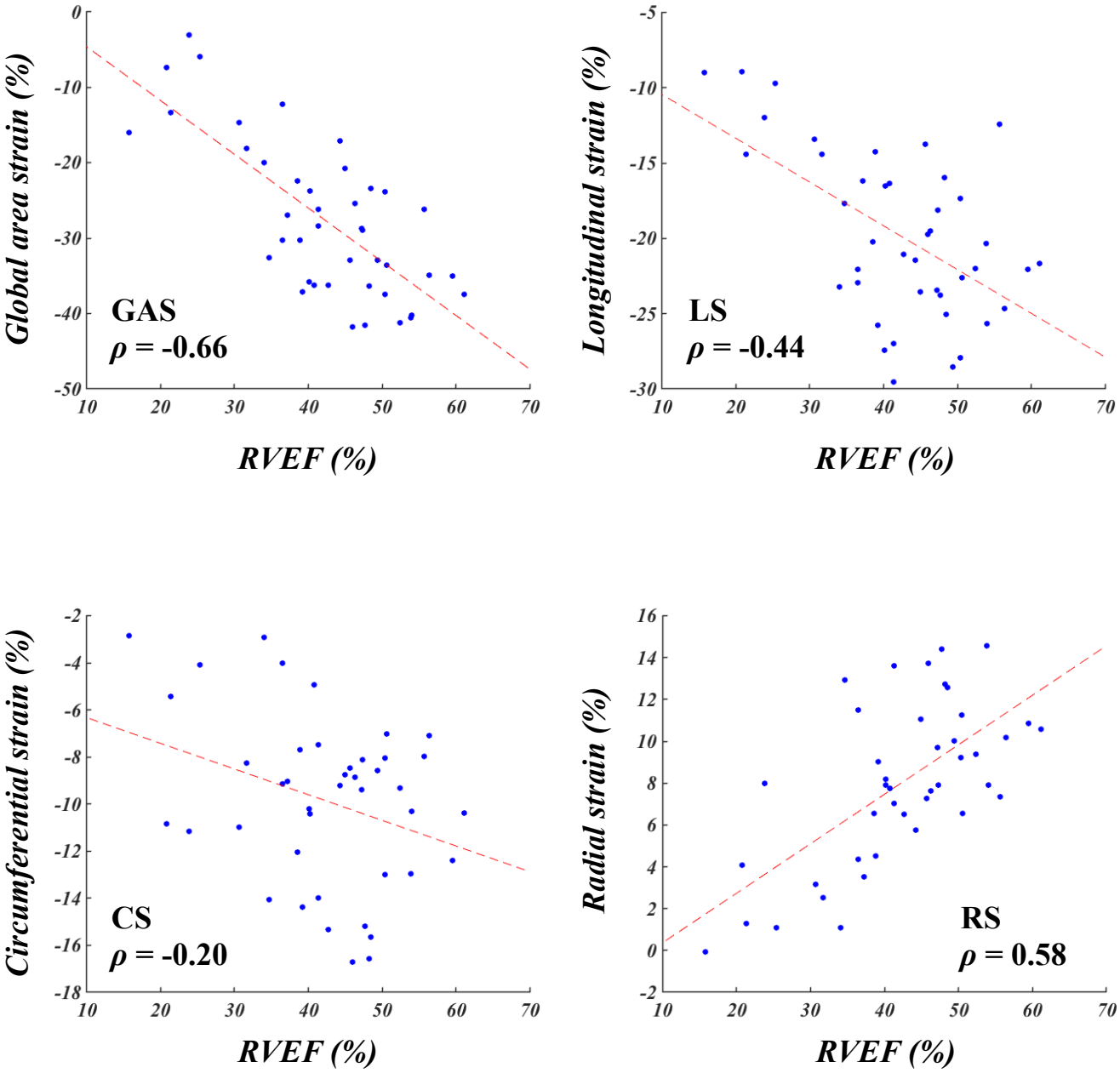

Correlations between right ventricular ejection fraction (RVEF) and global area strain (GAS), longitudinal strain (LS), circumferential strain (CS), and radial strain (RS). GAS, LS, and RS were significantly correlated with RVEF. No significant correlation could be identified between CS and RVEF. These plots include strain values before and after balloon pulmonary angioplasty (BPA).

Compliance with ethical standards:

Guarantor:

The scientific guarantor of this publication is Hiroshi Honda.

Conflict of interest:

The authors of this manuscript declare no relationships with any companies, whose products or services may be related to the subject matter of the article.

Funding:

This study has received funding by JSPS KAKENHI Grant Number JP16K19860.

Statistics and biometry:

No complex statistical methods were necessary for this paper.

Informed consent:

Only if the study is on human subjects:
Written informed consent was obtained from all subjects (patients) in this study.

Ethical approval:

Institutional Review Board approval was obtained.

Study subjects or cohorts overlap:

Some study subjects or cohorts have not been previously reported.

Methodology:

- retrospective
- observational
- performed at one institution